DOI: https://doi.org/10.17816/EID627123

Clinical cases of legionelliosis in the Krasnodar region during the new coronavirus infection COVID-19 pandemic: difficulties in diagnosis

Marina G. Avdeeva[1], Lyudmila P. Blazhnyaya[1], Dar'ya Yu. Moshkova[1], Makka I. Kulbuzheva[1, 2], Ilina M. Savitskaya[2], Angelina A. Podsadnyaya[1, 2], Natalya A. Kirilenko[1, 2], Elena E. Yakovchuk[2], Oksana V. Chernyavskaya[2], Polina O. Mamonova[2]

[1] Kuban State Medical University, Krasnodar, Russia;
[2] Specialized Clinical Infectious Diseases Hospital, Krasnodar, Russia

ABSTRACT

The high incidence of community-acquired pneumonia during the COVID-19 pandemic requires early differential diagnosis because of the differences in patient management techniques. Among community-acquired pneumonias, legionelliosis deserves special attention. The difficulty of clinical diagnosis of legionellosis during the COVID-19 pandemic leads to untimely prescription of specific antibacterial therapy, which worsens the prognosis. This study presents clinical examples that draw the attention of specialists to the clinical, laboratory, and radiological features of legionellosis and to the important role of epidemiological data in the differential diagnosis of legionellosis with COVID-19.

A feature of the described clinical cases was as follows: late diagnosis with hospitalization on days 7–10 of illness in patients with increased body mass index, severe bilateral polysegmental pneumonia with the formation of a cavity and multirow bullae in the lungs, presence of proteinuria, increased levels of urea and/or creatinine, and lymphopenia. In all cases, the patients had history of staying in air-conditioned rooms and traveling by train. Compute tomography diagnostics described a localization that is not typical for COVID-19, manifestation from areas of consolidation with a symptom of air bronchography, presence of pleural effusion, discrepancy between the intensity of changes from the disease onset, and severity of the patient's condition.

For the specific diagnosis of legionellosis, testing for *Legionella spp*. To determine the legionella antigen in the urine is recommended upon hospital admission for all patients with severe community-acquired pneumonia.

Keywords: legionellosis; clinic; diagnostics; computed tomography scan; COVID-19; case report.

To cite this article:
Avdeeva MG, Blazhnyaya LP, Moshkova DYu, Kulbuzheva MI, Savitskaya IM, Podsadnyaya AA, Kirilenko NA, Yakovchuk EE, Chernyavskaya OV, Mamonova PO. Clinical cases of legionelliosis in the Krasnodar region during the new coronavirus infection COVID-19 pandemic: difficulties in diagnosis. *Epidemiology and Infectious Diseases.* 2024;29(2):151–164. DOI: https://doi.org/10.17816/EID627123

Received: 17.02.2024 **Accepted:** 07.03.2024 **Published online:** 09.04.2024

DOI: https://doi.org/10.17816/EID627123

Случаи легионеллёза в Краснодарском крае в период пандемии новой коронавирусной инфекции COVID-19: трудности диагностики

М.Г. Авдеева[1], Л.П. Блажняя[1], Д.Ю. Мошкова[1], М.И. Кулбужева[1, 2], И.М. Савицкая[2], А.А. Подсадняя[1, 2], Н.А. Кириленко[1, 2], Е.Е. Яковчук[2], О.В. Чернявская[2], П.О. Мамонова[2]

[1] Кубанский государственный медицинский университет, Краснодар, Россия;
[2] Специализированная клиническая инфекционная больница, Краснодар, Россия

АННОТАЦИЯ

Высокая заболеваемость внебольничными пневмониями на фоне сохраняющейся регистрации COVID-19 требует проведения ранней дифференциальной диагностики ввиду различной тактики ведения пациентов. Среди внебольничных пневмоний особого внимания заслуживают заболевания легионеллёзной природы. Сложность клинической диагностики легионеллёза в период пандемии COVID-19 ведёт к несвоевременному назначению специфической антибактериальной терапии, что ухудшает прогноз исхода заболевания. В работе приведены клинические примеры, обращающие внимание специалистов на особенности клинико-лабораторных и рентгенологических проявлений легионеллёза, а также на важную роль эпидемиологических данных для дифференциальной диагностики легионеллёза с новой коронавирусной инфекцией COVID-19.

Особенностью описанных клинических случаев является: поздняя диагностика с госпитализацией на 7–10-й день болезни у пациентов, имеющих повышенный индекс массы тела; тяжёлое течение двусторонней полисегментарной пневмонии с формированием полости и многорядных булл в лёгких; наличие протеинурии, повышение уровня мочевины и/или креатинина, лимфопения. Во всех случаях отмечено нахождение в кондиционируемых помещениях, в том числе поездка в поезде. При КТ-диагностике описана нетипичная для COVID-19 локализация процесса, манифестация с участков консолидации с симптомом воздушной бронхографии, наличие плеврального выпота, несоответствие интенсивности изменений дню заболевания и тяжести состояния пациента.

Для специфической диагностики легионеллёза тестирование на *Legionella spp.* с определением легионеллёзного антигена в моче рекомендуется проводить при поступлении в стационар всем пациентам с тяжёлой внебольничной пневмонией.

Ключевые слова: легионеллёз; клиника; диагностика; компьютерная томография; COVID-19; клинический случай.

Как цитировать:
Авдеева М.Г., Блажняя Л.П., Мошкова Д.Ю., Кулбужева М.И., Савицкая И.М., Подсадняя А.А., Кириленко Н.А., Яковчук Е.Е., Чернявская О.В., Мамонова П.О. Случаи легионеллёза в Краснодарском крае в период пандемии новой коронавирусной инфекции COVID-19: трудности диагностики // Эпидемиология и инфекционные болезни. 2024. Т. 29, № 2. С. 151–164. DOI: https://doi.org/10.17816/EID627123

Рукопись получена: 17.02.2024 **Рукопись одобрена:** 07.03.2024 **Опубликована online:** 09.04.2024

ЭКО•ВЕКТОР

INTRODUCTION

In addition to continuous reports of new COVID-19 cases, high incidence of community-acquired pneumonia and severe acute respiratory infections necessitates early differential diagnosis due to differences in patient management strategies. Among community-acquired pneumonias, *Legionella* infections warrant particular attention. The challenges in clinical diagnosis of legionellosis during the COVID-19 pandemic lead to the delayed prescription of targeted antibacterial therapy, which worsens the prognosis of the disease outcome.

Legionellosis is known to manifest in two distinct forms, including a mild, acute respiratory disease, a domestic outbreak of which was first described in 1988 in Armavir city. The second one is severe pneumonia (Legionnaires' disease), which presents with pronounced intoxication, severe disorders of the central nervous system and kidneys, and a mortality rate of up to 10% [1, 2]. The sporadic incidence of legionellosis presents a challenge for clinical diagnosis, as physicians may lack the necessary vigilance and may be unaware of the specific clinical manifestations of the disease. The differential diagnosis of pneumonias of other bacterial and viral etiologies became more challenging during the COVID-19 pandemic. The severe course of *Legionella* pneumonia, which presents with clinical manifestations similar to those observed in lung damage associated with COVID-19, necessitates prompt diagnosis and early initiation of etiotropic antibiotic therapy.

In 2022, four patients hospitalized at the Specialized Clinical Infectious Diseases Hospital (SCIDH) of the Ministry of Health of the Krasnodar Region (Russia) with suspected SARS-CoV-2 infection were diagnosed with legionellosis. This report presents the three most illustrative clinical cases.

CASES DESCRIPTION

Case No. 1

Patient B, a 46-year-old female, was admitted to the SCIDH in Krasnodar on July 15, 2022, on day 11 of the disease. The patient presented with a fever (up to 38 °C), sore throat, cough with scanty sputum, exertional dyspnea, and chest discomfort.

Anamnesis morbi. On July 5, 2022, the patient exhibited acute symptoms of weakness, malaise, sore throat, and body temperature of 37.5 °C. On the following day, cough with scanty sputum also developed, and the temperature rose to 38.5 °C. The general practitioner prescribed umifenovir 200 mg four times a day and amoxicillin + clavulanic acid 2 g daily. During the therapy, fever persisted, reaching 39 °C daily. Additionally, the patient self-administered non-steroidal anti-inflammatory drugs. On day 7 of the disease, the patient began to experience chest discomfort and exertional dyspnea. At the second visit, the general practitioner recommended to add intramuscular ceftriaxone. A computed tomography (CT) scan of the chest was performed.

Description of the chest CT scan dated July 15, 2022 (Fig. 1*a*, 2*a*, 3*a*): The lungs are fully expanded. Pneumatization is diffusely reduced. The pulmonary pattern is deformed. Both lungs show multifocal infiltrative changes of the pulmonary

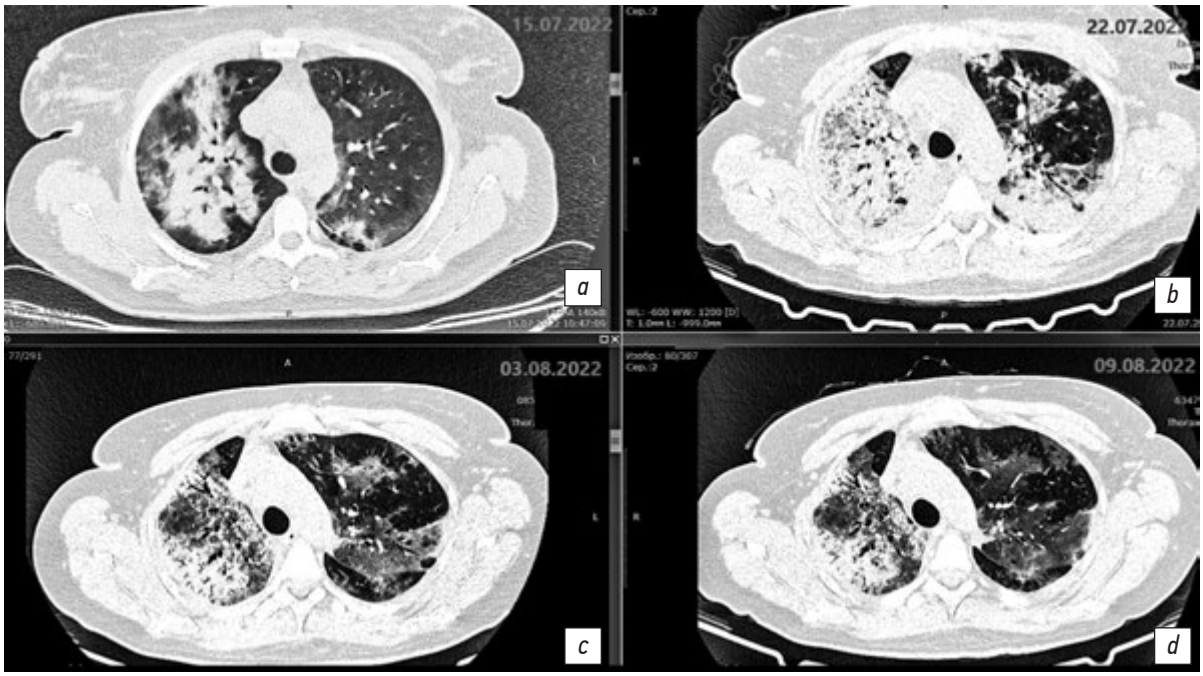

Fig. 1. Axial sections at the level of the aortic arch, pulmonary window. Changes in the areas of heterogeneous infiltration: *a*: chest CT scan dated July 15, 2022, day 11 of the disease, day 1 of hospitalization; *b*: chest CT scan dated July 22, 2022, day 18 of the disease, day 7 of hospitalization; *c*: chest CT scan dated August 3, 2022, day 30 of the disease, day 19 of hospitalization; *d*: chest CT scan dated August 9, 2022, day 36 of the disease, day 25 of hospitalization.

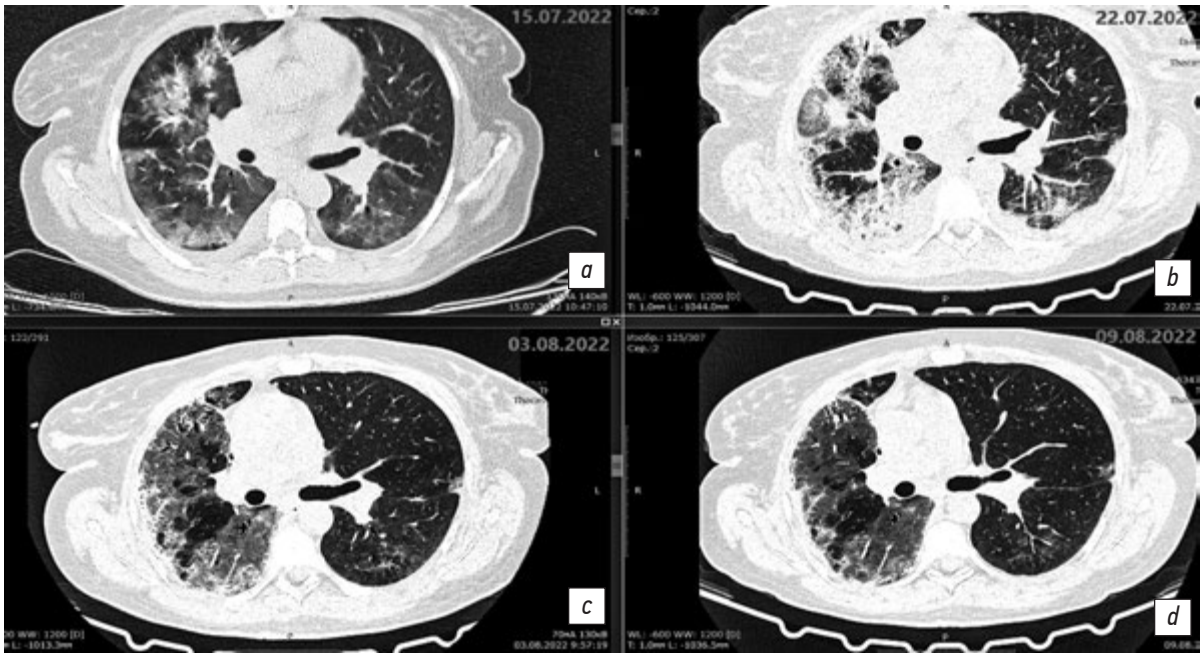

Fig. 2. Axial sections at the level of the main bronchi, pulmonary window. Changes in the areas of heterogeneous infiltration: *a*: chest CT scan dated July 15, 2022, day 11 of the disease, day 1 of hospitalization; *b*: chest CT scan dated July 22, 2022, day 18 of the disease, day 7 of hospitalization; *c*: chest CT scan dated August 3, 2022, day 30 of the disease, day 19 of hospitalization; *d*: chest CT scan dated August 9, 2022, day 36 of the disease, day 25 of hospitalization.

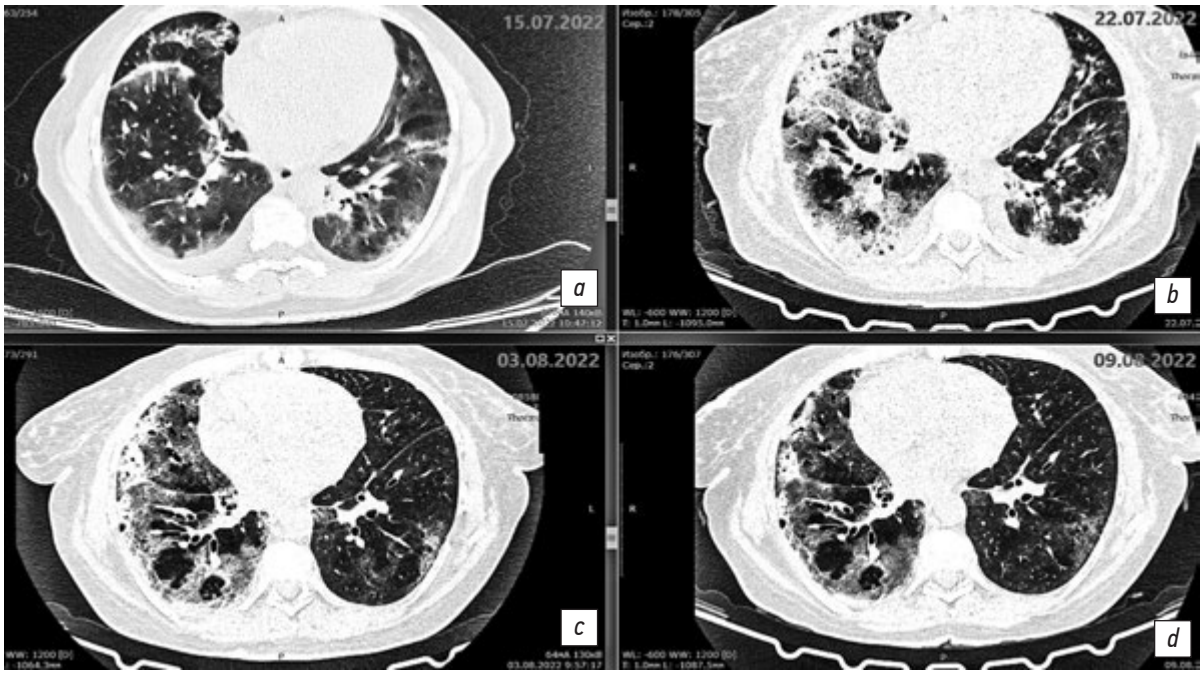

Fig. 3. Axial sections at the level of the basal parts of the lungs, pulmonary window. Changes in the areas of heterogeneous infiltration. *a*: chest CT scan dated July 15, 2022, day 11 of the disease, day 1 of hospitalization; *b*: chest CT scan dated July 22, 2022, day 18 of the disease, day 7 of hospitalization; *c*: chest CT scan dated August 3, 2022, day 30 of the disease, day 19 of hospitalization; *d*: chest CT scan dated August 9, 2022, day 36 of the disease, day 25 of hospitalization.

parenchyma of a ground-glass type with reticular shadows and peribronchial consolidation type. The infiltrative changes are located randomly. The parenchyma is visibly involved. Up to 30% and 60% of the pulmonary parenchyma is affected in the left upper and lower lobes, respectively. Up to 60% of the pulmonary parenchyma is affected in the right upper and lower lobes. The volume of the affected parenchyma in the left lung is up to 45% and less than 70% in the right lung. The total percentage of lung damage reaches 70%. The degree of severity is at the CT3 level.

The configuration and lumen of the trunk bronchi are unremarkable. The mediastinum is of normal shape and location. A layer of free fluid, up to 20 mm in thickness, is observed in the upper aortic pouch. The intrathoracic lymph nodes are indurated and enlarged. The para-aortic group is 11 mm along the short axis, the paratracheal group is up to 12 mm, the bifurcation group is up to 17 mm, and both bronchopulmonary groups are up to 12 mm. The major vessels are of normal structural organization and sizes. In both pleural cavities, a layer of free fluid is observed, measuring up to 15 mm along the posterior wall on the right side and up to 5 mm on the left side. *Results*: Bilateral multifocal pneumonia, intermediate probability of COVID-19 pneumonia (pneumonia of other etiology?), CT3, 65%–70%. Enlarged mediastinal lymph nodes, hydropericardium, bilateral hydrothorax, and focal mass in the left breast.

On the evening of July 15, 2022, day 11 of the disease, the patient's condition deteriorated. The patient called the emergency medical team and was admitted to a COVID hospital on oxygen support of 5 L/min with saturation of 93%–94%. The rapid test for COVID-19 was negative.

Epidemiologic history. The patient received the Gam-COVID-Vac vaccine against the SARS-CoV-2 infection at the beginning of the year. However, no vaccines against influenza or pneumococcus were administered. The patient was in an air-conditioned environment both at work and at home. Additionally, the patient's vehicle was equipped with air conditioner.

Anamnesis vitae. The patient denies chronic somatic diseases. A cholecystectomy was performed approximately 20 years ago (for cholelithiasis), and a total hysterectomy was conducted 7 years ago (for myoma).

Results of physical, laboratory, and instrumental tests

Upon admission on July 15, 2022, the patient was in severe condition, which was attributed to intoxication, respiratory syndromes, and respiratory failure. The CURB-65 (Confusion, Urea, Respiratory Rate, Blood Pressure, Age ⩾65) score of the patient was 0. The patient was conscious, responsive, and oriented. Meningeal signs were negative. The Glasgow Coma score was 15, and the Richmond Agitation-Sedation Scale (RASS) score was 0. The oropharyngeal mucosa was hyperemic, the tongue was moist and covered with white plaque. Auscultation revealed diminished breath sounds in the lungs over the entire chest surface. Additionally, rales were heard in the lower and middle parts of both lungs, and accessory muscles did not participate in respiratory movements. The skin was of normal color, with no evidence of rash. Subcutaneous adipose tissue was moderately developed. Physical status: height 172 cm, weight 87 kg, and BMI 29.4 kg/m^2. Air saturation was 88% and 96% with humidified insufflation at 6 L/min. The subject's heart rate (HR) was 76 bpm, and blood pressure was 124/80 mmHg. Diuresis was preserved and adequate.

Laboratory examination on the day of hospitalization revealed marked leukocytosis (WBC 24.1 × 10^9/L) and 4% lymphopenia (1.29 × 10^9/L); anemia (RBC 3.55 × 10^{12}/L, hemoglobin 112.0 g); thrombocytosis (544 × 10^9/L), hypoalbuminemia (23.9 g/L); increased lactate dehydrogenase (LDH) 634 U/L and C-reactive protein (CRP) 324.4 mg/L. Aspartate aminotransferase levels reached a maximum of 49 U/L, whereas alanine aminotransferase values remained within the normal range at 18 U/L. Additionally, electrolyte imbalances were observed (potassium ion 3.7 mmol/L, chloride 98 mmol/L, and calcium 1.07 mmol/L). The patient's procalcitonin level was 2.78 ng/mL, as determined by enzyme-linked immunosorbent assay (ELISA). Urinalysis: proteinuria (0.2 g/L), minor bacteriuria (+), leukocyturia (up to 7/HPF), unchanged erythrocytes (up to 16/HPF), squamous epithelium (up to 12), and unchanged urea (5.7 mmol/L) and creatinine (86 μmol/L). Activated partial thromboplastin time: 24 sec, prothrombin time: 18.4 sec, prothrombin index (PTI): 48.1%, international normalized ratio: 1.56, fibrinogen: 6.3 g/L, thrombin time: 16.5 sec, and D-dimer: 1.88 mg/L.

Given the negative immunochromatography result for SARS-CoV-2 antigens, polymerase chain reaction (PCR) tests for influenza A (H1N1), influenza A, influenza B, and legionellosis viruses were performed to confirm the diagnosis. Two hours after admission to the hospital, *Legionella* antigens were detected in the urine using the immunochromatographic method.

Clinical diagnosis: Legionellosis (severe). Community-acquired bilateral multifocal pneumonia (severe). Complications: Respiratory failure (grade 2), bilateral hydrothorax, hydropericardium, and overweight with a BMI of 29.4 kg/m^2.

Interventions. Etiotropic therapy included intravenous levofloxacin 500 mg twice a day and intravenous azithromycin 500 mg once a day, in combination with enoxiparin sodium and humidified insufflation. On July 19, 2022, no positive changes required therapy adjustment. Azithromycin was replaced with intravenous rifampicin 600 mg once a day.

The patient's condition remained severe over two weeks. Febrile fever persisted, accompanied by weakness, exertional dyspnea, paroxysmal dry cough, chest discomfort, rales in the lower and middle parts of both lungs, and a negative water balance (3,600 mL injected, 2750 mL excreted) on some days. Laboratory tests demonstrated a gradual decline in leukocytosis, reaching 16.7 × 10^9/L, accompanied by increased thrombocytosis, reaching 983 × 10^9/L, and toxic neutrophil granularity (++). On July 22, 2022, *Candida albicans* was isolated from the oropharynx. Consequently, fluconazole and inhalation therapy with budesonide and furosemide were added to the therapy. Repeated bacteriologic blood and urine flora tests for differential diagnosis were negative.

On day 18 of the disease and day 7 of the hospital stay, the chest CT scan dated July 22, 2022 (Fig. 1*b*, 2*b*, 3*b*) revealed negative changes in bilateral multifocal pneumonia and weakly negative changes in bilateral pneumothorax and hydropericardium. Moderate intrathoracic lymphadenopathy

without changes and a focal mass in the left breast were observed. Antibiotic therapy was re-adjusted; rifampicin was discontinued, and intravenous tigecycline 100 mg daily was added to levofloxacin 1 g daily. This regimen demonstrated gradual positive changes.

Since August 1, 2022 (day 28 of the disease, day 17 of inpatient treatment), the patient's condition was of average severity, with normalized body temperature, decreased symptoms of respiratory insufficiency, and persistent weakness. The air saturation was 89% and 97% with humidified insufflation at 4 L/min. The chest CT scan dated August 3, 2022 revealed mixed changes of bilateral multifocal pneumonia. The left lung exhibited positive findings, whereas the right lung displayed cavitary lesions. The presence of a dilated bronchial lumen and heterogeneous infiltration were suspected. The regression of bilateral hydrothorax was accompanied by negative changes in hydropericardium.

Description of the chest CT scan dated August 3, 2022 (Fig. 1*c*, 2*c*, 3*c*): The lung volume increased due to regression of fluid in the pleural cavities on both sides. Previously, the maximum fluid level was 21 mm on the right side and up to 19 mm on the left side, with a flow along the interlobular pleura up to 17 mm. Multiple segments of the lungs exhibit extensive confluent areas of heterogeneous infiltration, predominantly of the consolidation type. Within these areas, the lumen of dilated bronchi and a ground glass appearance is observed, accompanied by a single discoid atelectasis. The changes have no preferred localization. A marked continuous reduction in the extent and intensity of changes in the left lung is observed, with preserved ground-glass changes and consolidation (S1/2).

The extent of changes in the right lung remains unaltered. However, an increase in consolidation is observed in the upper regions. Additionally, heterogeneous infiltration in the right lung in S6 and S10 segments caused cavitary lesions up to 9 × 7 mm and 4 × 5 mm, respectively. This phenomenon is likely attributable to the dilation of the bronchial lumen, heterogeneous expansion of infiltration, or the formation of a destruction cavity.

The paratracheal lymph nodes are 12 mm in diameter, whereas the bifurcation lymph nodes measure up to 14 × 18 mm (previously 17 × 22 mm). The heart is unremarkable. Fluid in the pericardial cavity supradiaphragmatically is up to 14 mm (previously 10 mm). A focal mass is present in the upper-inner quadrant of the left breast, measuring up to 11 mm, with a density of 22 HU, and insufficiently clear contours. *Results*: Bilateral multifocal pneumonia with mixed changes (positive in the left lung). Cavitary lesions in the right lung may be characterized by dilated bronchial lumen, heterogeneous infiltration, or a destruction cavity. Follow-up chest CT is recommended. There is evidence of bilateral hydrothorax regression. The hydropericardium shows negative changes. Moderate intrathoracic lymphadenopathy exhibits weakly positive changes. A focal mass in the left breast is observed.

The antibiotic therapy was continued at the same dosage, prophylaxis of thromboembolic events was administered, and periodic oxygen therapy was provided.

On August 10, 2022 (day 37 of the disease, day 26 of hospitalization), the patient's condition was deemed satisfactory. The patient reported a rare dry cough and slight exertional dyspnea. The patient's air saturation was 97%. The chest CT scan dated August 9, 2022 (Fig. 1*d*, 2*d*, 3*d*) demonstrated positive changes in bilateral multifocal pneumonia, with a decrease in intensity. Additionally, there were no changes in cavitary lesions in the right lung, which could be attributed to dilated bronchial lumen or heterogeneous infiltration. Hydropericardium also showed positive changes.

Outcome and results of follow-up

The patient was discharged with clinical improvement of pneumonia, residual asthenia, and respiratory syndrome and was referred for further outpatient follow-up. A consultation with an oncologist and a hematologist was recommended, as well as a follow-up chest CT scan.

DISCUSSION 1

Although the diagnosis was established on the first day of hospitalization following a negative result of the SARS-CoV-2 test and identification of *Legionella* antigen in the urine, the disease was severe and prolonged. Negative factors include late hospitalization (on day 11 of the disease) and prehospital administration of drugs ineffective against legionellosis. The initial diagnosis of legionellosis may be challenging due to CT findings similar to those of viral pneumonia associated with SARS-CoV-2. Furthermore, the atypical localization of the pathological process in the lungs, manifested by consolidation areas with air bronchogram, and pleural effusion should be noted. Comorbidities (CT finding of a mass in the breast) in conjunction with excessive body weight and high thrombocytosis may contribute to the disease severity, resulting in bilateral multifocal pneumonia with the formation of a destruction cavity in the lungs, hydrothorax, and hydropericardium.

Case No. 2

A 27-year-old patient was admitted to the SCIDH in Krasnodar on July 24, 2022, on day 7 of the disease, with complaints of increased body temperature, chills, cough, and dyspnea.

Anamnesis morbi. The symptoms occurred on July 18, 2022 and included chills, body aches, and body temperature of 37.5 °C. On the subsequent day, the patient exhibited sore throat, weakness, body temperature of 38.5 °C, rare dry cough, and chest discomfort. On day 6 of the disease, July 23, 2022, onset of exertional dyspnea and increased cough were noted. The patient self-administered oseltamivir, azithromycin

500 mg daily, and nimesulide. Testing for SARS-CoV-2 yielded a negative result. On the following day (July 24, 2022), a chest CT scan was performed as the condition deteriorated. It revealed bilateral multifocal pneumonia with 60% lung damage and intrathoracic lymphadenopathy. Given the suspicion of a severe coronavirus infection, the patient was transported by ambulance to SCIDH. The results of the rapid test and PCR for SARS-CoV-2 performed in the hospital were negative.

Epidemiologic history. The patient resides in an apartment with his parents, who are in good health. He has not traveled outside the region. The apartment is equipped with an AC system. No vaccinations against SARS-CoV-2, influenza, or pneumococcus were administered.

Anamnesis vitae. The patient reports no previous history of illness.

Results of physical, laboratory, and instrumental tests

Upon admission, the patient's condition was assessed as severe. The CURB-65 score was 0. The severity of the patient's condition was attributed to a pronounced intoxication syndrome, respiratory syndrome, respiratory failure, and asthenia. The patient oriented to place and time and had no meningeal signs or focal symptoms. The Glasgow score was 15, and the Richmond Agitation-Sedation Scale (RASS) score was 0. The skin was pale, subcutaneous adipose tissue was moderately developed. Physical status: height 170 cm, weight 82 kg, and BMI 28.4 kg/m^2. Nasal breathing was clear. Accessory muscles did not participate in respiratory movements; respiratory rate (RR) was 18 per minute; air saturation was 93% and 96%–97% with humidified insufflation at 3 L/min and decreased to 91% during physical activity. Auscultation revealed diminished breath sounds in the lungs over the entire chest surface. Additionally, rales were heard in the lower parts of both lungs. The pulse rate was 85 per minute, while the blood pressure was 123/80 mm Hg. The abdomen was soft, non-tender, and moderately enlarged due to subcutaneous adipose tissue. The liver and spleen were not enlarged, no CVA tenderness on both sides. Diuresis was adequate to the amount of fluid intake. In view of the initial negative result for coronavirus infection, a test for legionellosis, mycoplasmosis, chlamydia, and influenza was scheduled for differential diagnosis.

Laboratory results obtained upon admission: WBC 8.47 × 10^9/L, lymphopenia (0.64 × 10^9/L); increased LDH 640 U/L, CRP 400 mg/L, glucose 7.6 mmol/L, ferritin 761.8 μg/L, creatinine 112 μmol/L, fibrinogen 13.4 g/L, and D-dimer 4 mg/L. The patient's PTI was 65.7%, the lactate level was 3.72 mmol/L, and the procalcitonin (ELISA) level was 1.024 μg/L. The urea level remained within the normal range of 5.5 mmol/L. Urinalysis revealed proteinuria (3.5 g/L), acetone (++), bile pigments, renal epithelium (up to 4/HPF), WBCs (up to 5/HPF), altered erythrocytes (up to 5/HPF), and single cylinders in the HPF. Three hours after admission to the hospital, a positive urinalysis result was obtained for *Legionella* antigen by immunochromatographic method.

Clinical diagnosis: Legionellosis (severe). Community-acquired bilateral multifocal pneumonia.

Interventions. Antibiotic treatment included a combination of levofloxacin 1.0 g daily and azithromycin 500 mg daily administered intravenously for 7 days, followed by oral therapy, in conjunction with ipratropium bromide and fenoterol inhalation therapy and humidified insufflation.

The therapy improved the patient's general condition and laboratory parameters. Body temperature, coagulation and urinalysis parameters returned to normal, oxygen saturation reached 98%, WBC 4.57 × 10^9/L, lymphocytes 0.94 × 10^9/L, glucose 6.0 mmol/L, LDH 385 U/L. Chlamydia and mycoplasma were not detected.

Description of the chest CT scan dated August 2, 2022, on day 16 of the disease, day 9 of hospitalization (Fig. 4, 5, 6):

Fig. 4. Axial section, pulmonary window. Small bullae with ground glass areas. Day 16 of the disease, day 9 of hospitalization.

Fig. 5. Axial section, pulmonary window. Bilateral areas of low-intensity ground glass. Day 16 of the disease, day 9 of hospitalization.

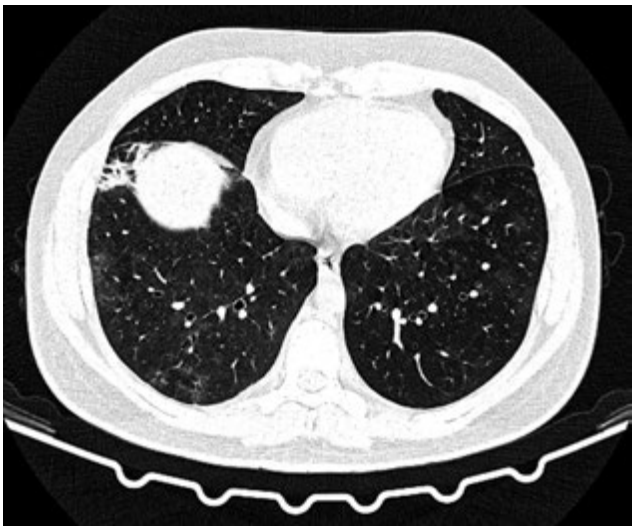

Fig. 6. Axial section, pulmonary window. Thickened area in S8 of the right lung. Day 16 of the disease, day 9 of hospitalization.

The lungs are fully expanded. In subpleural sections S1, S3, and S5 of the right lung and S1/2 and S3 of the left lung, grouped small multi-row bullas together with areas of ground-glass type hypoventilation are observed. There are areas of heterogeneous infiltration, predominantly of low-intensity ground-glass type, in multiple foci of both lungs. In the subpleural sections of S8 of the right lung, dense consolidation is detected. The changes are not preferentially localized, with the greatest severity in the subpleural regions. Degrees of pathological changes in each lobe are as follows: right lung: upper lobe 20%, middle lobe 60%, lower lobe 40%–45%; left lung: upper lobe 15%–20%; lower lobe 25%–30%. The total lesion is thus 45%–50%.

Results: CT pattern of a bilateral infiltration, intermediate probability of viral etiology (CT2, 45%–50%); small bullas in both lungs. The effective equivalent dose is 1.908 m3v.

Final diagnosis: Legionellosis (severe). Community-acquired multifocal pneumonia (severe). Respiratory failure (grade 1).

Outcome and results of follow-up. The patient was discharged with improvement in condition on day 12 of hospitalization and day 19 of the disease and was referred for outpatient treatment.

DISCUSSION 2

Severe disease with bilateral multifocal pneumonia and small bullas in both lungs was observed in a young man with no chronic co-morbidities. Among the identified risk factors, only overweight was present. Additionally, high inflammation parameters, including CRP, ferritin, D-dimer, marked lymphopenia, and a renal reaction, were noted. Azithromycin at the outpatient stage was beneficial, but did not prevent the severe course of the disease. CT revealed the lesions at locations atypical for SARS-CoV-2 infection, mainly in subpleural areas. Additionally, the intensity of the observed changes were inconsistent with the disease course and severity of the patient's condition.

Case No. 3

Patient L., a 65-year-old male, was admitted to SCIDH on day 5 of the disease, on May 15, 2022, with symptoms of weakness, malaise, decreased appetite, elevated body temperature up to 40 °C, occasional cough with clear sputum, exertional dyspnea, and chest discomfort.

Anamnesis morbi. On May 11, 2022, the subject exhibited acute illness manifested by weakness, malaise, drowsiness, chills, and fever reaching 39.2 °C. In the following days, body temperature rose to 39.6 °C, accompanied by rare cough with clear sputum, decreased appetite, and a single episode of vomiting after eating. The patient did not seek medical assistance and instead self-administered paracetamol, Rengalin, and umifenovir. On day 5 of the disease, the patient's condition deteriorated; weakness and fatigue increased, body temperature elevated up to 40 °C, exertional dyspnea and chest discomfort occurred. The patient was transported by ambulance to the central district hospital in Goryachiy Klyuch. A rapid test for SARS-CoV-2 yielded a negative result. Chest CT scan revealed bilateral multifocal interstitial pneumonia, a high risk of SARS-CoV-2 infection, and a stage of progression consistent with the average lesion volume, classified as CT2. The lesion volume in the right and left lungs was 20% and 25%, respectively. Given the possible diagnosis of COVID-19 and oxygen saturation of 95%, the patient was transferred to SCIDH in Krasnodar.

Epidemiologic history. The patient resides in Goryachiy Klyuch in a private residence with his wife, who is in good health. One week prior to the onset of symptoms, the patient traveled by train to Rostov-on-Don for a two-day period. No vaccinations against influenza, novel coronavirus infection, or pneumococcus were administered.

Anamnesis vitae. The patient has hypertension and is unable to provide blood pressure data.

Results of physical, laboratory, and instrumental tests

Upon admission to SCIDH, the patient's condition was moderately severe, attributable to intoxication and respiratory syndromes. The CURB-65 score was 2. The patient was conscious, adequately oriented, and exhibited asthenia. The Glasgow score was 15, and the RASS score was 0. subcutaneous adipose tissue was moderately developed. Physical status: weight 78 kg, height 160 cm, and BMI 30.5. The skin was of normal color, and accessory muscles did not participate in respiratory movements. RR was 18 per minute, and oxygen saturation was 95%. The heart rhythm was regular, with pulse of 86 bpm and blood pressure of 115/70 mm Hg. The abdomen was soft, non-tender upon palpation, the liver and spleen were not enlarged. Moderate

coronavirus infection was suspected as a preliminary diagnosis. Complications: Bilateral multifocal pneumonia (not severe). No respiratory failure. Concomitant pathologies: Hypertension, grade 1 obesity.

Laboratory results obtained upon admission: leukocytosis (12.39×10^9/L), lymphopenia (0.70×10^9/L), CRP 445.2 mg/L, urea 11.9 mmol/L, creatinine 197 μmol/L, sodium 135.7 mmol/L, potassium 4.3 mmol/L, ferritin 613.8 μg/L, LDH 371 U/L, glucose 11.3 mmol/L, and procalcitonin 8.74 ng/mL.

Description of the chest CT scan dated May 15, 2022, on day 5 of the disease, day 1 of hospitalization. The lungs are fully expanded. In S2 of the right lung (subtotally with marked reticular changes) and in S1/2 and S6 segments of the left lung, subpleural confluent areas of heterogeneous infiltration of consolidation type with a peripheral rim of ground glass are observed, with bronchial lumen visible in the affected S2 segment of the right lung. Focal masses with somewhat radial contours, measuring up to 3.8 × 5.1 mm and 7.9 × 6.2 mm, are observed in the upper S2 segment on the right side. Degrees of pathological changes in each lobe are as follows: right lung: upper lobe 35%, middle lobe 0%, lower lobe 0%; left lung: upper lobe 10%; lower lobe 15%–20%. The total lesion is approximately 20%. The bronchial lumen is patent, and the intrathoracic or axillary lymph nodes are not enlarged. There are minimal amounts of free fluid in the pleural cavities on both sides, with the largest quantity observed on the right side at 5–6 mm and on the left side at 2–4 mm. The heart is unremarkable. *Results*: CT pattern of bilateral multifocal pneumonia with intermediate probability of viral etiology (CT1, approximately 20%). Focal masses in the right lung warrants a follow-up examination. Minor bilateral hydrothorax.

Interventions. Antiviral therapy included favipiravir 3,600 mg daily, intramuscular ceftriaxone 2.0 g daily, captopril for blood pressure increase, prophylaxis of thromboembolic events, proning, and humidified insufflation. During the two-day treatment, the patient's condition remained unchanged, with body temperature up to 39.8 °C, RR 19 per minute, blood pressure 120/60 mm Hg, and oxygen saturation 95%.

On May 17, 2022, a negative result of the PCR RNA SARS-CoV-2 test and a positive result of the *Legionella* antigen test in urine by immunochromatographic method were obtained. The diagnosis of coronavirus infection was revised to moderate legionellosis, mild bilateral multifocal pneumonia and no respiratory failure. The therapy was adjusted. Favipiravir and ceftriaxone were discontinued; intravenous levofloxacin 1.0 g daily, sodium heparin 20,000 U daily, diuretics, inhalation with ambroxol 2.0 mL (7.5 mg/mL) twice daily, and insufflation with humidified oxygen were initiated.

On May 18, 2022, day 3 of hospitalization, negative changes were observed due to increasing intoxication and respiratory syndromes, as well as onset of respiratory failure (oxygen saturation: 90%, RR: 22 per minute). Humidified insufflation with a flow rate of 6 L/min was connected, resulting in saturation of 95%. Clinical diagnosis: Legionellosis (severe course), bilateral multifocal pneumonia (severe), respiratory failure (grade 1). Follow-up chest CT was performed.

Description of the chest CT scan dated May 18, 2022, day 8 of the disease, day 3 of hospitalization (Fig. 7*a*, 8*a*). The lungs display negative infiltrative changes, with increasing extent and size, and new infiltration areas occurred in the lower lobe of the right lung. The lungs are fully expanded. Multiple segments of the lungs exhibit extensive confluent areas of heterogeneous infiltration of the consolidation type with a peripheral rim of ground glass are observed, with visible bronchial lumen. Focal masses with somewhat radial contours, measuring up to 3.8 × 5.1 mm and 7.9 × 6.2 mm, are observed in the upper S2 segment on the right side. The bronchial lumen is patent, and the intrathoracic or axillary lymph nodes are not enlarged. Free fluid in the pleural cavities is observed on both sides. On the right side, the fluid extends up to 7–8 mm (previously 5–6 mm), whereas

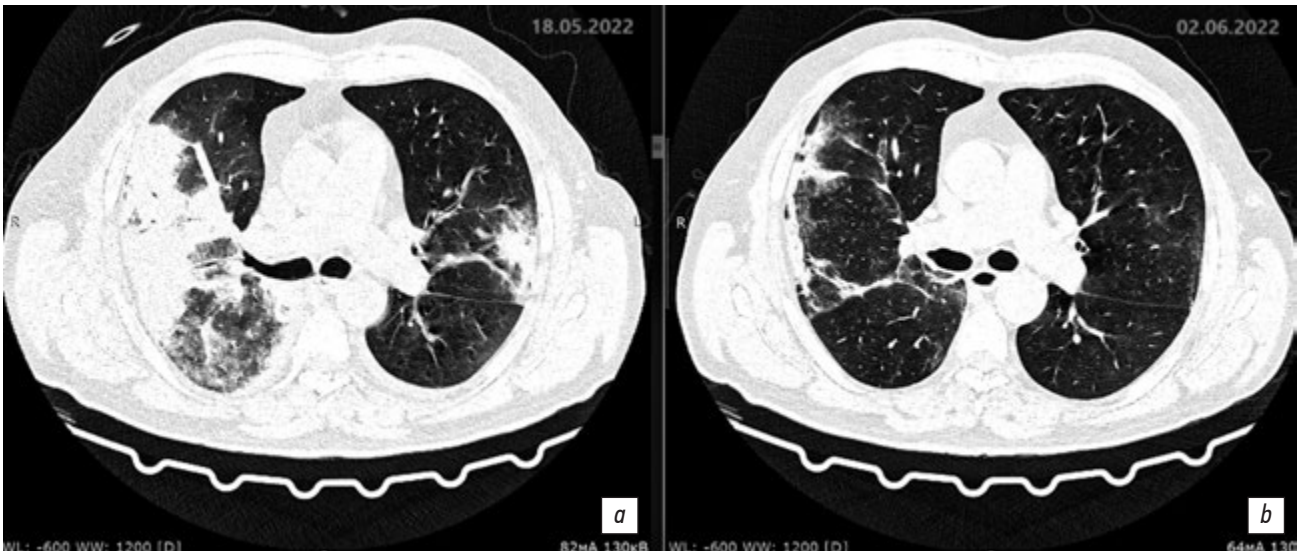

Fig. 7. Axial sections showing changes at the level of the upper parts of the lungs over time, pulmonary window: *a*: chest CT scan dated May 18, 2022, day 8 of the disease, day 3 of hospitalization; *b*: chest CT scan dated June 2, 2022, day 23 of the disease, day 17 of hospitalization.

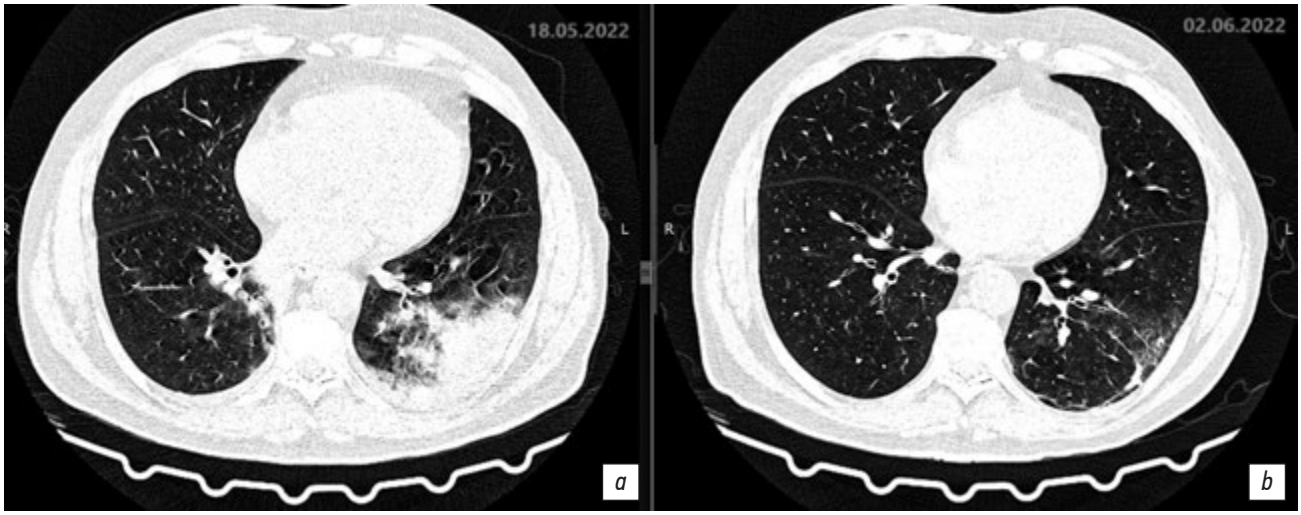

Fig. 8. Axial sections showing changes at the level of the lower parts of the lungs over time, pulmonary window: *a*: chest CT scan dated May 18, 2022, day 8 of the disease, day 3 of hospitalization; *b*: chest CT scan dated June 2, 2022, day 23 of the disease, day 17 of hospitalization.

on the left side, the fluid reaches up to 6 mm (previously 2–4 mm). The heart is unremarkable. *Results*: CT pattern of negative changes in bilateral multifocal pneumonia and bacterial disease (legionellosis?). Focal lesions in the right lung without changes and minor bilateral hydrothorax with slightly negative changes.

The therapy was adjusted to add intravenous azithromycin 500 mg daily. Levofloxacin and azithromycin were continued for a period of 14 days. Gradual improvement was observed. On day 17 of the disease, May 28, 2022, the patient's condition was of moderate severity, the improvement was due to decreased respiratory failure symptoms. Blood chemistry results improved: CRP 6.0 mg/L, urea 4.7 mmol/L creatinine 89 μmol/L, WBC 6.5 × 10^9/L, and lymphocytes 3.8 × 10^9/L.

Description of the chest CT scan dated June 2, 2022, day 23 of the disease, day 17 of hospitalization (Fig. 7*b*, 8*b*). Compared to the previous CT scan on May 18, 2022, there is a notable improvement in the extent, size, and intensity of infiltration in the lungs. The lungs are fully expanded. Multiple segments of the lungs show rare confluent areas of heterogeneous infiltration, characterized by heavy consolidation and ground glass appearance. Focal masses with somewhat radial contours, measuring up to 3.8 × 5.1 mm and 7.9 × 6.2 mm, are observed in the upper S2 segment on the right side. The bronchial lumen is patent, and the intrathoracic or axillary lymph nodes are not enlarged. Free fluid in the pleural cavities on both sides remains undetermined (previously noted on the right up to 7–8 mm, on the left up to 6 mm). The heart is unremarkable.

Results: CT pattern of positive changes of bilateral multifocal pneumonia (stage of incomplete resolution). Focal lesions in the right lung. Follow-up is recommended. Minor bilateral hydrothorax shows positive changes.

Outcome and results of follow-up. On June 3, 2022 (day 24 of the disease and day 18 of hospitalization), the patient's condition was satisfactory. The patient presented with complaints of marked general weakness and dry cough and was discharged with recovery from the underlying disease, residual asthenia and respiratory syndrome; outpatient follow-up was recommended. Recommendations included a chest CT scan in 1 and 6 months and a pulmonologist consultation based on the results.

DISCUSSION 3

In this case, a 65-year-old male patient with a history of hypertension, first degree obesity, and transient hyperglycemia, in addition to bilateral multifocal pneumonia with focal masses in the lungs and bilateral hydrothorax, had abnormal urinalysis results (proteinuria, leukocyte presence, and microhematuria), increased urea and creatinine levels. These findings suggested potential influence of concomitant disorder on renal function and the association with the underlying disease. CT scan revealed an atypical localization of the process, manifested by consolidation areas, air bronchogram, and pleural effusion.

CONCLUSION

Challenges in diagnosing legionellosis given current high incidence of COVID-19 is attributed to similar clinical symptoms during the first days of both diseases. They include fever, sore throat, chest discomfort, weakness, dry cough or cough with scanty sputum, dyspnea, and CT signs of bilateral multifocal pneumonia. Remarkably, not all patients had clinically significant signs of renal damage, which is an important consideration for the diagnosis of legionellosis. However, proteinuria and abnormalities in the urine sediment were observed in all cases. The young patient with no co-morbidities had an elevated creatinine level in conjunction with a normal urea level. In the patient with concomitant hypertension, both urea and creatinine levels were increased.

Amoxicillin + clavulanic acid and ceftriaxone during the first days of the disease were found to have no effect. Cephalosporin antibiotics did not improve the patient's condition, nor prevent a severe course of the disease with the development of acute respiratory failure. This is because these drugs have no effect on intracellular bacteria, such as *Legionella*. The late diagnosis at the outpatient stage and failure of the initial therapy resulted in the increasing severity of the patient's condition and delayed hospitalization.

Legionella species are facultative intracellular pathogens. *Legionella* penetrates into the cytoplasm of alveolar macrophages via phagocytosis, forming a unique phagosome that does not fuse with lysosomes, resulting in incomplete phagocytosis. Active replication of *Legionella* occurs in the formed vacuole [3]. Currently, the detailed mechanism of *Legionella* pathogenicity is well studied. *Legionella pneumophila* is able to survive inside phagocytizing host cells, creating a special protected replication space, called the *Legionella*-containing vacuole (LCV). The success of LCV biogenesis and intracellular replication of the pathogen depend on the rapid evasion of the host cell's degradative antimicrobial pathways and the acquisition of nutrients necessary for bacterial growth. This is achieved through the synthesis of effector proteins by *Legionella*, which are incorporated into the LCV wall and translocated into the host cell cytosol [4]. For this process, *L. pneumophila* uses the Dot/Icm type IV secretion system (T4SS), which facilitates the transportation of over 300 different effector proteins into the host cell [5]. The T4SS complex was demonstrated to traverse the envelope of *Legionella* within the vacuole along the bacterial poles [6]. Consequently, *Legionella* adheres its cell pole to the LCV membrane.

In addition, the virulence of *Legionella* is associated with its ability to simultaneously hijack several molecular pathways of the host cell, particularly the ubiquitin system, using the advantages of both conventional and unconventional (phosphoribosyl-linked) ubiquitination, thus providing optimal conditions for replication [7]. The first line of defense against *Legionella* infection at early stages of the disease is innate immune responses, which are mediated by Toll-, NOD-, and RIG-I-like receptors. During the acute phase of *Legionella* infection, macrophages, neutrophils, natural killer (NK) cells, B cells, and CD4+ and CD8+ T cells migrate to the interstitial regions of the lungs. The activation of NK cells induces effector functions, including the secretion of cytokines and chemokines, and leads to the lysis of target cells in the lungs [8]. These processes are clinically manifested by powerful inflammatory reactions and the destruction of lung tissues, which explains the disease severity observed in the aforementioned clinical cases.

A clinically severe pneumonia with a marked intoxication syndrome and no epidemiologic history complicated by coronavirus infection allows the physician to suspect that the pneumonia may have a *Legionella* nature. Challenges of differential diagnosis are increased by low-specific changes in instrumental tests.

In cases of pneumonia caused by *Legionella*, the clinical presentation on CT scans is similar to that of viral pneumonia associated with SARS-CoV-2. This includes infiltrative changes of the ground-glass type and subsequent consolidation. However, the first and third clinical cases showed an atypical localization, manifested by consolidation areas with air bronchogram, and pleural effusion. In the second case, the location was atypical, and the intensity of the changes was inconsistent with the disease course and severity of the patient's condition.

The distinctive characteristics of the aforementioned clinical cases include delayed diagnosis with hospitalization on days 7–10 of the disease; severe disease, manifested by the development of bilateral multifocal pneumonia with formation of a cavity and multilobular bullas in the lungs; proteinuria, elevated urea and/or creatinine levels, lymphopenia; and an increased BMI. In all cases, exposure to air-conditioned premises, including train travel, was reported.

A focused epidemiologic history, urinary changes such as acute nephritis, and early laboratory testing for urinary *Legionella* antigen will aid in the diagnosis of legionellosis. Testing for *Legionella* spp. is recommended to be conducted in all patients presenting with severe community-acquired pneumonia upon admission to the hospital.

Considering the intracellular replication of *Legionella*, the therapy should include antibiotics that effectively penetrate the intracellular space [9]. The recommended first-line therapy is fluoroquinolones (levofloxacin or moxifloxacin) or macrolides (preferably azithromycin). Our observations indicate that the desired effect was achieved with a combination of levofloxacin and azithromycin. Inadequate or delayed antibiotic treatment of legionellosis is associated with worse prognosis [10]. Therefore, antibiotics targeted against *Legionella* spp. are recommended to be included in empirical therapy at early stages of severe community-acquired pneumonia.

ADDITIONAL INFORMATION

Funding source. This study was not supported by any external sources of funding.

Competing interests. The authors declare that they have no competing interests.

Authors' contribution. All authors made a substantial contribution to the conception of the work, acquisition, analysis, interpretation of data for the work, drafting and revising the work, final approval of the version to be published and agree to be accountable for all aspects of the work. M.G. Avdeeva, L.P. Blazhnyaya, D.Yu. Moshkova, M.I. Kulbuzheva, I.M. Savitskaya, A.A. Podsadnyaya, N.A. Kirilenko, E.E. Yakovchuk, O.V. Chernyavskaya, P.O. Mamonova — development of the concept and implementation of the work, preparation and editing of the text of the article, approval of the final version of the article.

Consent for publication. Written consent was obtained from the patients for publication of relevant medical information and all of accompanying images within the manuscript in Epidemiology and Infectious Diseases Journal.

REFERENCES

1. Cattan S, Thizy G, Michon A, et al. Actualités sur les infections à Legionella. *Rev Med Interne*. 2019;40(12):791–798. (In French). doi: 10.1016/j.revmed.2019.08.007

2. Graham FF, Hales S, White PS, Baker MG. Review Global seroprevalence of legionellosis — a systematic review and meta-analysis. *Sci Rep*. 2020;10(1):7337. doi: 10.1038/s41598-020-63740-y

3. Chauhan D, Shames SR. Pathogenicity and Virulence of Legionella: Intracellular replication and host response. *Virulence*. 2021;12(1):1122–1144. doi: 10.1080/21505594.2021.1903199

4. Kim S, Isberg RR. The Sde phosphoribosyl-linked ubiquitin transferases protect the Legionella pneumophila vacuole from degradation by the host. *Proc Natl Acad Sci U S A*. 2023; 120(33):e2303942120. doi: 10.1073/pnas.2303942120

5. Shames SR. Eat or Be Eaten: Strategies Used by Legionella to Acquire Host-Derived Nutrients and Evade Lysosomal Degradation. *Infect Immun*. 2023;91(4):e0044122. doi: 10.1128/iai.00441-22

6. Böck D, Hüsler D, Steiner B, Medeiros JM, Welin A, Radomska KA, Hardt WD, Pilhofer M, Hilbi H. The Polar Legionella Icm/Dot T4SS Establishes Distinct Contact Sites with the Pathogen Vacuole Membrane. *mBio*. 2021;12(5):e0218021. doi: 10.1128/mbio.02180-21

7. Tomaskovic I, Gonzalez A, Dikic I. Ubiquitin and Legionella: From bench to bedside. *Semin Cell Dev Biol*. 2022;132:230–241. doi: 10.1016/j.semcdb.2022.02.008

8. Park B, Park G, Kim J, Lim SA, Lee KM. Innate immunity against Legionella pneumophila during pulmonary infections in mice. *Arch Pharm Res*. 2017;40(2):131–145. doi: 10.1007/s12272-016-0859-9

9. Chahin A, Opal SM. Severe Pneumonia Caused by Legionella pneumophila: Differential Diagnosis and Therapeutic Considerations. *Infect Dis Clin North Am*. 2017;31(1):111–121. doi: 10.1016/j.idc.2016.10.009

10. Viasus D, Gaia V, Manzur-Barbur C, Carratalà J. Legionnaires' Disease: Update on Diagnosis and Treatment. *Infect Dis Ther*. 2022;11(3):973–986. doi: 10.1007/s40121-022-00635-7

СПИСОК ЛИТЕРАТУРЫ

1. Cattan S., Thizy G., Michon A., et al. Actualités sur les infections à Legionella // Rev Med Interne. 2019. Vol. 40, N 12. P. 791–798. doi: 10.1016/j.revmed.2019.08.007

2. Graham F.F., Hales S., White P.S., Baker M.G. Review Global seroprevalence of legionellosis — a systematic review and meta-analysis // Sci Rep. 2020. Vol. 10, N 1. P. 7337. doi: 10.1038/s41598-020-63740-y

3. Chauhan D., Shames S.R. Pathogenicity and Virulence of Legionella: Intracellular replication and host response // Virulence. 2021. Vol. 12, N 1. P. 1122–1144. doi: 10.1080/21505594.2021.1903199

4. Kim S., Isberg R.R. The Sde phosphoribosyl-linked ubiquitin transferases protect the Legionella pneumophila vacuole from degradation by the host // Proc Natl Acad Sci U S A. 2023. Vol. 120, N 33. P. e2303942120. doi: 10.1073/pnas.2303942120

5. Shames S.R. Eat or Be Eaten: Strategies Used by Legionella to Acquire Host-Derived Nutrients and Evade Lysosomal Degradation // Infect Immun. 2023. Vol. 91, N 4. P. e0044122. doi: 10.1128/iai.00441-22

6. Böck D., Hüsler D., Steiner B., et al. The Polar Legionella Icm/Dot T4SS Establishes Distinct Contact Sites with the Pathogen Vacuole Membrane // mBio. 2021. Vol. 12, N 5. P. e0218021. doi: 10.1128/mbio.02180-21

7. Tomaskovic I., Gonzalez A., Dikic I. Ubiquitin and Legionella: From bench to bedside // Semin Cell Dev Biol. 2022. Vol. 132. P. 230–241. doi: 10.1016/j.semcdb.2022.02.008

8. Park B., Park G., Kim J., Lim S.A., Lee K.M. Innate immunity against Legionella pneumophila during pulmonary infections in mice // Arch Pharm Res. 2017. Vol. 40, N 2. P. 131–145. doi: 10.1007/s12272-016-0859-9

9. Chahin A., Opal S.M. Severe Pneumonia Caused by Legionella pneumophila: Differential Diagnosis and Therapeutic Considerations // Infect Dis Clin North Am. 2017. Vol. 31, N 1. P. 111–121. doi: 10.1016/j.idc.2016.10.009

10. Viasus D., Gaia V., Manzur-Barbur C., Carratalà J. Legionnaires' Disease: Update on Diagnosis and Treatment // Infect Dis Ther. 2022. Vol. 11, N 3. P. 973–986. doi: 10.1007/s40121-022-00635-7

AUTHORS' INFO

*** Marina G. Avdeeva**, MD, Dr. Sci. (Medicine), Professor;
address: 4 Sedin street, 350063 Krasnodar, Russia;
ORCID: 0000-0002-4979-8768;
eLibrary SPIN: 2066-2690;
e-mail: avdeevam@mail.ru

Lyudmila P. Blazhnyaya, MD,
Cand. Sci. (Medicine), Associate Professor;
ORCID: 0000-0002-0055-1764;
eLibrary SPIN: 1164-7038;
e-mail: lp-blazhnyaya@mail.ru

Dar'ya Yu. Moshkova, MD, Cand. Sci. (Medicine),
Associate Professor;
ORCID: 0000-0003-1401-6970;
eLibrary SPIN: 9489-0057;
e-mail: mrs_darya@mail.ru

ОБ АВТОРАХ

*** Авдеева Марина Геннадьевна**, д-р мед. наук, профессор;
адрес: Россия, 350063, Краснодар, ул. Седина, д. 4;
ORCID: 0000-0002-4979-8768;
eLibrary SPIN: 2066-2690;
e-mail: avdeevam@mail.ru

Блажняя Людмила Павловна,
канд. мед. наук, доцент;
ORCID: 0000-0002-0055-1764;
eLibrary SPIN: 1164-7038;
e-mail: lp-blazhnyaya@mail.ru

Мошкова Дарья Юрьевна,
канд. мед. наук, доцент;
ORCID: 0000-0003-1401-6970;
eLibrary SPIN: 9489-0057;
e-mail: mrs_darya@mail.ru

Makka I. Kulbuzheva, MD, Cand. Sci. (Medicine), Associate Professor;
ORCID: 0000-0003-1817-6664;
eLibrary SPIN: 8090-3715;
e-mail: kulbuzhevamakka@yandex.ru

Ilina M. Savitskaya, MD;
ORCID: 0009-0004-5818-5287;
eLibrary SPIN: 1479-9720;
e-mail: savitskaya-ilina@yandex.ru

Angelina A. Podsadnyaya, MD;
ORCID: 0009-0009-5225-9296;
eLibrary SPIN: 8490-1523;
e-mail: podsadnyaya.lina@mail.ru

Natalya A. Kirilenko, MD;
ORCID: 0000-0003-2302-6214;
e-mail: dr.kirilenko-1978@mail.ru

Elena E. Yakovchuk;
ORCID: 0009-0001-9690-7285;
e-mail: elena-yakovchuk@yandex.ru

Oksana V. Chernyavskaya;
ORCID: 0009-0007-8032-3537;
e-mail: kdlskib@mail.ru

Polina O. Mamonova, MD;
ORCID: 0009-0002-6945-7263;
e-mail: polinadoncova@yandex.ru

Кулбужева Макка Ибрагимовна,
канд. мед. наук, доцент;
ORCID: 0000-0003-1817-6664;
eLibrary SPIN: 8090-3715;
e-mail: kulbuzhevamakka@yandex.ru

Савицкая Илина Михайловна;
ORCID: 0009-0004-5818-5287;
eLibrary SPIN: 1479-9720;
e-mail: savitskaya-ilina@yandex.ru

Подсадняя Ангелина Александровна;
ORCID: 0009-0009-5225-9296;
eLibrary SPIN: 8490-1523;
e-mail: podsadnyaya.lina@mail.ru

Кириленко Наталья Алексеевна;
ORCID: 0000-0003-2302-6214;
e-mail: dr.kirilenko-1978@mail.ru

Яковчук Елена Евгеньевна;
ORCID: 0009-0001-9690-7285;
e-mail: elena-yakovchuk@yandex.ru

Чернявская Оксана Викторовна;
ORCID: 0009-0007-8032-3537;
e-mail: kdlskib@mail.ru

Мамонова Полина Олеговна;
ORCID: 0009-0002-6945-7263;
e-mail: polinadoncova@yandex.ru

* Corresponding author / Автор, ответственный за переписку